16th World Conference on Earthquake, 16WCEE 2017
Santiago Chile, January 9th to 13th 2017
Paper N° 2075
Registration Code: S-C1461631137

A CASE STUDY: APPLICATION OF THE HARDNESS METHOD TO ESTIMATE THE RESIDUAL CAPACITY OF REINFORCEMENT IN AN EARTHQUAKE DAMAGED BUILDING

G. Loporcaro[(1)], S. Pampanin[(2)], M.V. Kral[(3)]

[(1)] *PhD Candidate, University of Canterbury, giuseppe.loporcaro@pg.canterbury.ac.nz*
[(2)] *Professor, University of Canterbury, stefano.pampanin@canterbury.ac.nz*
[(3)] *Professor, University of Canterbury, milo.kral@canterbury.ac.nz*

1. Abstract

Capacity design and hierarchy of strength are at the base of modern seismic codes which allow an inelastic response of structures in case of severe earthquakes. Therefore, in traditional reinforced concrete (RC) structures damage develops in defined locations known as plastic hinges. As expected, during the 2010 and 2011 Christchurch earthquakes, plastic hinges formed in beams, coupling beams and at the base of columns and walls preventing collapse. However, structures were damaged permanently.

Due to the lack of literature on methods to evaluate the residual capacity of damage buildings to sustain subsequent aftershocks and on reliable and cost-efficient repairing techniques to bring back the structure "at least" as it was before the earthquake, a significant number of multi-storey RC buildings were deemed irreparable and were demolished.

New Zealand local authorities and industry have request to develop techniques for assessing damage to steel reinforcement bars embedded in concrete elements. Immediately following the 2010/2011 Christchurch earthquakes, low invasive techniques able to quantify the level and extent of plastic deformation and residual plastic capacity were not available.

The current method (known as "in situ hardness method") is based on measuring hardness with a Leeb hardness portable device in situ then correlating it to plastic strain based upon laboratory tensile tests. Extensive studies and practical applications have been conducted soon after the Christchurch earthquakes, but the in situ method has not yet been vetted in the open literature, and thus has not been widely accepted.

In the present work, based on empirical relationships between hardness versus strain and residual strain capacity, a damage assessment procedure is presented. If damage is found in situ via Leeb hardness testing, a bar may be removed for more accurate hardness measurements in lab using the Vickers hardness methodology. The Vickers hardness profile of damaged bars is then compared with calibration curves (Vickers hardness versus strain and residual strain capacity) developed for the same steel reinforcement (grade and diameter) extracted from undamaged locations.

The paper presents the findings of experimental tests conducted to estimate strain and residual strain capacity of damaged locations in individual bars in earthquake damaged buildings. The proposed methodology also accounts for the effects of strain ageing, which should not be ignored. Note also that this testing is entirely monotonic (not cyclic).

Keywords: steel reinforcing bar, residual capacity, hardness, damage assessment, strain ageing

1. Introduction

Designing a building to withstand severe earthquakes elastically is not economically convenient, therefore seismic codes allow for the damage of structures. At the ultimate limit state, “ordinary” structures are designed to prevent collapse, therefore designers can reduce seismic forces based on the overall ductility and redundancy of the entire structural system. As a result, structures are expected to survive to the design-level earthquake at the cost of permanent damage as a consequence of large inelastic deformation and energy dissipation of the structural material [1].

Capacity design and the hierarchy of strength philosophy which are at the base of modern seismic codes encourages structural engineers to locate and detail plastic hinges in order to act as a ductile “fuse”. In the case of a high intensity seismic event, plastic hinges are expected to dissipate energy and prevent unwanted brittle failure mechanisms [1]. During an earthquake, in reinforced concrete (RC) structures, the steel reinforcement plays a fundamental role: it dissipates energy through the hysteresis loop. In addition, reinforcement have the ability to sustain load cycles that induce to high plastic deformation without reduction in strength. Plastic hinges undergo high level of cyclic plastic rotations that induce large flexural compressive and tensile stresses in the concrete and steel causing permanent damage. As observed by numerous laboratory tests, a uniform crack distribution pattern, (Fig. 1) spread over the plastic hinge zone, is expected [2] [3]. However, during the Canterbury earthquakes, in some cases only few large cracks were observed [2].

In the 2010 and 2011 seismic sequence, RC buildings in the Christchurch CBD were subjected to high levels of seismic acceleration. The associated seismic demand was beyond that predicted for the 500-year return period design spectrum by the current standard NZS 1170.5:2004 [4] [2] [3] [5]. As result, many RC structural elements experienced large inelastic deformations [6] and in ductile RC concrete buildings plastic hinges formed in the expected structure locations: beams, coupling beams and at the base of columns and walls manifested as cracking and permanent plastic deformation of the steel reinforcement (see Fig. 1) [3].

During the post-earthquake assessment phase, territorial authorities, insurance companies and private engineering firms required information regarding the reparability of buildings. In the case of RC structures, information was needed about the damage state of the steel reinforcing bars. However, at that stage there was no widely accepted practice to determine the extent of damage in the steel and the residual strain capacity or ductility.

Fig. 1 Beam plastic hinges in a 22-storey reinforced concrete building constructed in mid-end 1980s [3].

2. Previous work on determining damage to structural and reinforcement steel

Techniques to quantify the plastic deformation in structural steel and reinforcement are not fully developed yet. The only few applications available in literature are based on hardness testing, as plastic deformation causes yield strength increase [7] [8] and yield strength can be correlated to hardness of metals [9]. An application on earthquake damaged structural steel, based on the relationship between hardness and plastic strain, was previously investigated by Matsumoto [10]. Tensile tests and hardness tests were conducted on Japanese SN490 structural steel beams in order to investigate the correlation between hardness and mechanical properties. Results showed that tensile strength increased with hardness, and uniform elongation decreased with increase in hardness.

An on-site testing method with minimal damage, also known “in situ hardness method”, was proposed more recently. The “in situ hardness method” correlates the hardness measured on site with a portable hardness testing device to plastic strain determined from laboratory tensile tests on the same or similar material [11] [12]. Practical applications were conducted soon after the Christchurch earthquakes in New Zealand. “In-situ” Leeb and lab-based Rockwell B hardness measurements were carried out on the Eccentrically Braced Frames (EBF) of the Pacific Tower in Christchurch [11]. Results showed an increase in Leeb and Rockwell B hardness in the web section of the active link beam of damaged EBFs compared to the undamaged steel. This increase was an indication of plastic deformation of the steel member. A Christchurch based engineering firm conducted damage assessment of some Christchurch RC buildings. Leeb hardness tests were carried out on site on steel reinforcement that crossed concrete cracks. The cover concrete was removed to expose the rebar. The exposed surface was ground flat and surface-finished to approximately 120 grit to allow for hardness testing. Leeb hardness measurements were performed at uniformly-spaced intervals along a length of the bar in order to identify any increase above the hardness baseline in the crack vicinity. In order to quantify the amount of plastic deformation, a correlation between Leeb hardness and steel plastic strain was determined through laboratory-based hardness and tensile tests [12].

3. Definition of hardness

Hardness has different meanings “depending upon the experience of the person involved” [7]. As a general definition, hardness provides information about the resistance of a metal to plastic deformation. In material testing, hardness is defined as the resistance of a metal against the penetration of a harder indenter such as a diamond or hard steel ball. In design applications, hardness is an easy and practical measure of the deformation resistance and provides information about the thermo-mechanical history of a metal [7].

The traditional hardness testing method is the static indentation method such as Brinell, Rockwell and Vickers hardness tests. A specific load is applied into the surface of a metal sample through a diamond/hard steel indenter, when equilibrium is reached the indentation surface area is measured with the aid of a microscope. Hardness is then obtained as load applied over indentation area. An alternative testing method is the rebound or dynamic hardness test, in which an impact spherical body is dynamically applied on a metal surface sample. Hardness is measured as energy dissipation during the impact. An example is the Leeb hardness test [13].

Over the last century many relationships between hardness and mechanical properties of metals such as yield strength, ultimate tensile strength (UTS) and strain at UTS were documented. Equations and details can be found elsewhere [9] [14] [15] [16] [17] [18].

4. Strain ageing

Many carbon steels are subjected to a time- and temperature-dependent "strain-ageing" phenomenon during *(dynamic strain ageing)* and after plastic deformation *(static strain ageing)* which causes a significant change in the mechanical properties of the steel, [19] [20] [21] [22]. This phenomenon is due to the diffusion of interstitial nitrogen and carbon atoms, which pin mobile dislocations in new positions after the steel has strained. This “pinning” effect becomes stronger as the ageing time increases and with higher nitrogen and carbon interstitial content [23]. Because of the relatively low diffusivity of carbon below 100°C, nitrogen is the main cause of strain ageing at “ambient” temperatures (~15°C). At these temperatures, natural strain ageing is relatively slow and increases with the temperature [24] [25].

Hundy [25] derived an equation between the time of ageing at room temperature and the time of ageing at elevated temperatures:

$$\log_{10}\frac{t_r}{t} = H\left(\frac{1}{T_r}-\frac{1}{T}\right) - \log_{10}\frac{T}{T_r} \quad (1)$$

t_r is the strain-ageing time at room temperature Tr (K), and t is the time (s) that produced the equivalent strain ageing effect at an elevated temperature T (K). The constant H is 4000 if it assumed that nitrogen atoms cause ageing, otherwise H is 4400 if it assumed that carbon atoms cause ageing.

Table 1, obtained from equation (1), correlates the equivalent ageing times at room to the time that cause equivalent strain ageing effects at elevated temperatures. Therefore, it possible to accelerate the strain ageing effects occurred in one year at 15°C ageing pre-strained samples at 100°C, for example in boiling water.

Table 1 Equivalent ageing times at various temperatures [25].

15°C	**21°C**	**100°C**
1 year	6 months	4 hours
6 months	3 months	2 hours
3 months	6 weeks	1 hour
1 month	2 weeks	20 min.
1 week	4 days	5 min.
3 days	36 hours	2 min.

The strain ageing phenomenon is illustrated in Fig. 2 for New Zealand Grade 300E [26]. Examine the example where a strain-ageing prone steel is loaded in tension beyond its elastic stress A. If the steel sample is unloaded and then immediately reloaded, the specimen will show elastic behaviour up to stress A and strain hardening will continue as if the test had not interrupted (grey line). No discontinuous yield stress will be observed. On the other hand, if the sample is unloaded, aged and then reloaded, the discontinuous yield point phenomenon will reappear at a higher stress (point B). In addition, the ultimate tensile strength will be higher and ductility will reduce. Strain ageing also causes an increase in the ductile-brittle transition temperature [21].

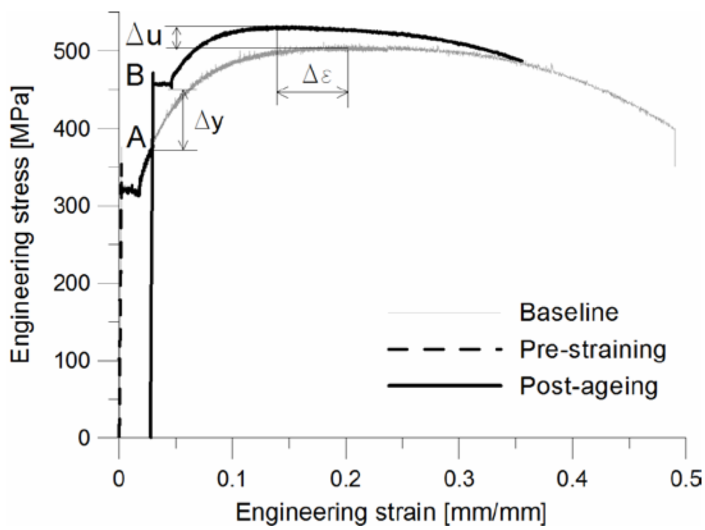

Fig. 2 Stress – strain curves of seismic Grade 300 reinforcing steel, as-received (un-aged), and pre-strained to 0.03mm/mm, aged for 4 hours at 100°C to simulate one year at 15°C and then re-loaded to investigate strain age effects.

Modern steel grades, such as NZ Grade 300E, are largely used in earthquake resistant structures because of their capacity to withstand large plastic deformation at plastic hinge locations. Experiments showed that these steel grades are susceptible to strain ageing effects [27] [24] [28], and that structures with such steel in damaged locations might have changed mechanical properties.

5. Limitations of previous works

A critical assessment conducted on previous works have demonstrated some limitations. The Leeb portable hardness testers used in some of the previous researches, based on the rebounding hardness testing method, might not represent an accurate method to measure the hardness of steel reinforcing bars. However, it can be reasonably used as an initial “filter” to identify which re-bars may require additional testing. The weight and thickness of the sample tested influence Leeb hardness readings [13], therefore ASTM A965-12 suggests a minimum test piece weight and a minimum thickness. Test pieces less than the minimum weight, as in the case of steel re-bars, require a rigid support and coupling to a thick and heavy element such as a steel plate. This can be obtain using specific coupling pastes as recommended by Leeb portable hardness manufacturers [29]. In Fig. 3 the Leeb and Vickers hardness versus plastic deformation relative to the same steel are compared. It can be clearly observed that Vickers hardness increases with the amount of pre-strain, the same is not true for Leeb hardness. Leeb hardness readings are also affected by a higher standard deviation.

For laboratory based hardness measurements, previous research [11] has correlated plastic strain to Rockwell hardness. For the strain range analysed in the present study it was found that the Rockwell hardness scale showed a limited resolution in comparison with Vickers (see Fig. 4 and Fig. 5).

Finally, because strain ageing increases the hardness of metals and decreases ductility it cannot be neglected as it was in previous applications.

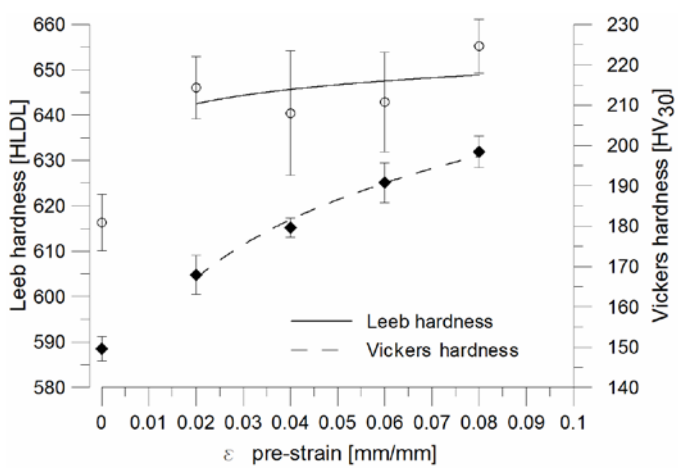

Fig. 3 Comparison Leeb and Vickers hardness versus pre-strain curves for NZ Grade 300E steel reinforcing bar.

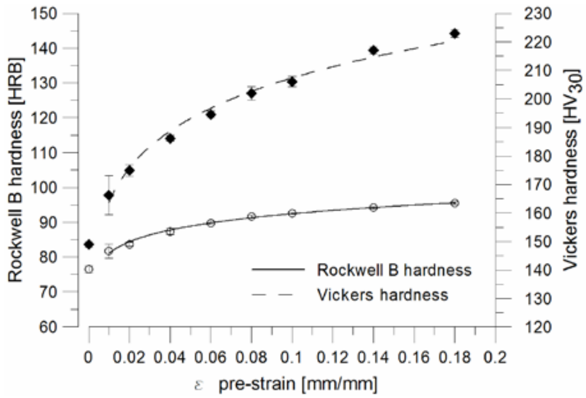

Fig. 4 Rockwell B and Vickers hardness versus pre-strain calibration curves for Grade 300E steel reinforcing bar.

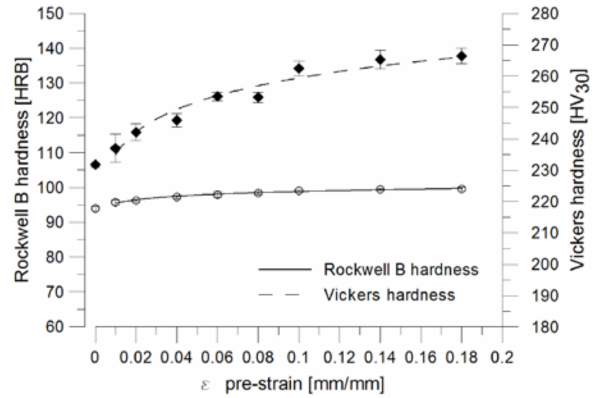

Fig. 5 Rockwell B and Vickers hardness versus pre-strain calibration curves for Grade 500E steel reinforcing bar.

6. Damage assessment

The hardness method is described through a case study of a Christchurch CBD building damaged during the 2010/2011 earthquakes sequence.

The process takes place over four phases:

I. Suspected damaged reinforcing bars are removed from the building;
II. Vickers hardness tests are conducted to detect the exact location of damage on the bars;
III. If and when damage is identified, calibration curves of that specific grade and diameter of steel are produced and used to estimate damage and predict residual plastic deformation capacity;
IV. Tensile tests of the damaged location are carried out and compared to tensile test of undamaged steel from the same bar.

During the first phase, based on visual inspection of earthquake damage, static residual crack width and structural analysis, structural engineers identified a number of locations in each building from where suspected damaged reinforcement had to be removed for further investigation. The exact location of a specific reinforcing bar crossing a crack was found using electro-magnetic devices. The cover concrete was then removed to expose the steel bar taking care to prevent further damage to the steel and finally removed for damage assessment in laboratory.

The results from two reinforcing bars, named as bar D1 and D2, will be used to describe the methodology. Diameter, average hardness in the un-damaged location and grades are presented in Table 2. The steel grade was determined based on mechanical properties obtained from laboratory testing, average hardness of the material in the undamaged region, existing drawings, construction date, bar mark indicating grade and relative steel reinforcing material standard.

Table 2 Basic initial information about the selected damaged reinforcing bars.

Bar name	**Diameter [mm]**	**Average hardness in the undamaged region [HV_{30}]**	**Grade**
D1	16	≈ 190	430
D2	25	≈ 145	300

Vickers hardness testing was conducted in phase II. The “suspected” damaged bars removed from the building were brought to the University of Canterbury for hardness testing. First, the bars were cut approximately into 150 mm lengths, with the crack location in the centre, to facilitate the surface preparation. The undamaged portion of the same bar was set aside for the final tensile testing (Phase IV). Two opposite sides of each bar section surface were ground flat and parallel using a water cooled grinder, sequentially ground from 180 to 600 grit using silicon carbide papers, and then finally polished to a 9-micron finish. Vickers hardness measurements were collected along the longitudinal section of the steel bar at 4 mm spacing (see Fig. 6), this was reduced to 2 mm when a hardness rise was detected.

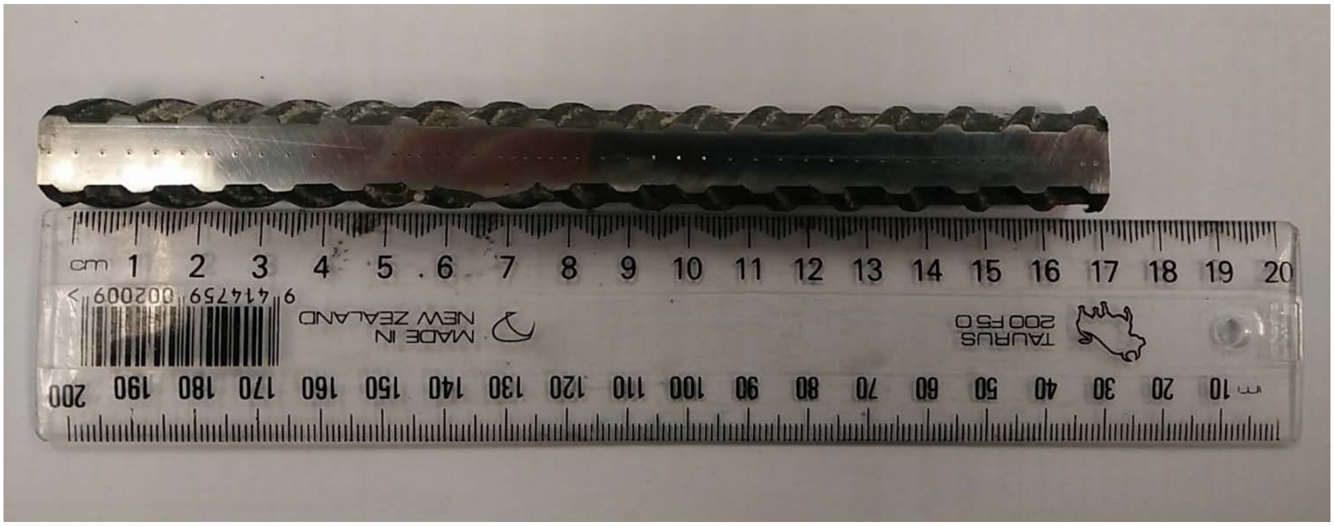

Fig. 6 - Vickers hardness indents shown on a typical polished surface.

A longitudinal hardness profile of the bars D1 and D2 are presented in Fig. 7 and Fig. 8. Bar D1 showed a rise above the baseline hardness of 190 HV_{30} over a region of approximately 160 mm averaging ≈ 197 HV_{30}; bar D2 exhibited an increase above the baseline hardness (150 HV_{30}) over almost the entire length of the bar, the average hardness in the central region of the sample (this will be used in phase IV as gauge length for tensile testing) was approximately 172 HV_{30}.

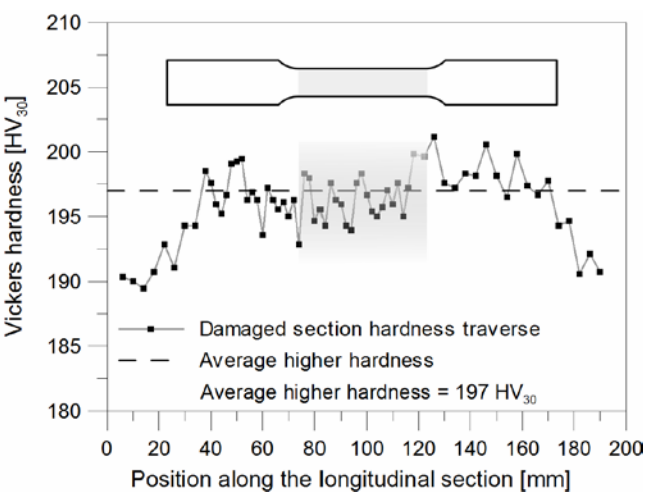

Fig. 7 - Vickers hardness traverse profile of the D1 damaged bar.

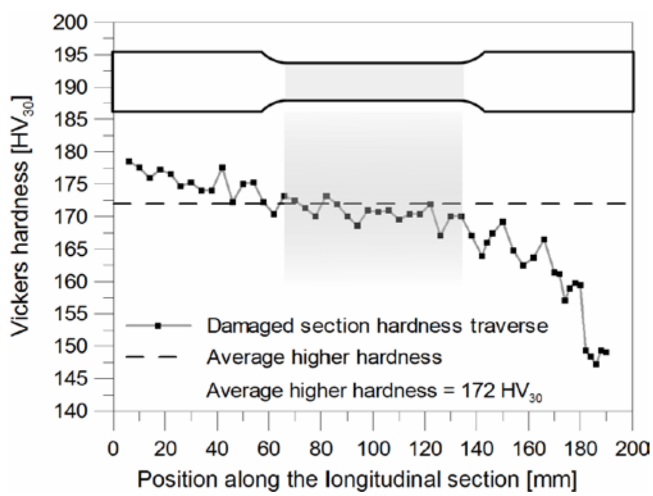

Fig. 8 - Vickers hardness traverse profile of the D2 damaged bar.

In phase III, two set of calibration curves were developed for steels of the same grade and diameter of sample D1 and D2. Hardness versus strain and hardness versus residual strain capacity were obtained by carrying out monotonic tensile tests to specific pre-strain levels, measuring the Vickers hardness at each pre-strain, followed by strain ageing, retesting the Vickers hardness and then monotonic tensile testing to failure.

In order to undertake the calibration testing, undamaged reinforcement of the same bar type and diameter and similar location/element as the damaged material were obtained. In order to provide twenty-one specimens required for the test approximately six meters of steel re-bar of diameter 16 mm (grade 430) and 25 mm (grade 300) were obtained. The specimens were machined to a “dog-bone” shape. Geometry and samples dimensions were defined according to the ASTM Standard E8/E8M - $11^{\varepsilon 1}$ [30].

From the 21 set of specimens, three samples were used to obtain the benchmark (unstrained and un-aged) mechanical properties: stress – strain curve, lower yield stress (YS), ultimate tensile strength (UTS), strain at UTS and Vickers hardness baseline (Table 3). Six pre-strain limits of 0.01, 0.02, 0.03, 0.04, 0.05 and 0.10 mm/mm were selected with three specimens for each pre-strain level. Strain ageing effects were investigating immersing the pre-strained specimens in boiling water (100°C) for four hours in order to simulate the one-year effect at 15°C.

The hardness versus plastic strain calibration curve (Fig. 9 and Fig. 11) and the residual strain capacity versus hardness calibration curve (Fig. 10 and Fig. 12) were obtained. The residual strain capacity is the strain corresponding to the ultimate tensile stress.

Table 3 - Average tensile properties of steel reinforcing bar for the selected bar group.

Diameter	**Grade**	**Lower Yield strength [MPa]**	**Ultimate tensile strength (UTS) [MPa]**	**Strain at UTS (%)**	**Vickers hardness baseline [HV_{30}]**
16	430	467	630	15.6	189
25	300	317	502	19.8	146

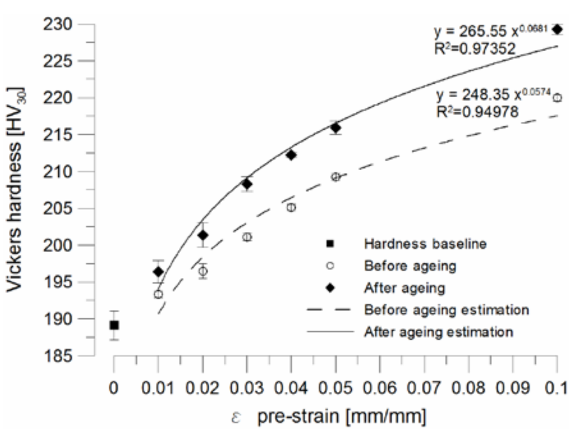

Fig. 9 Hardness versus pre-strain calibration curve for diameter 16 mm grade 430.

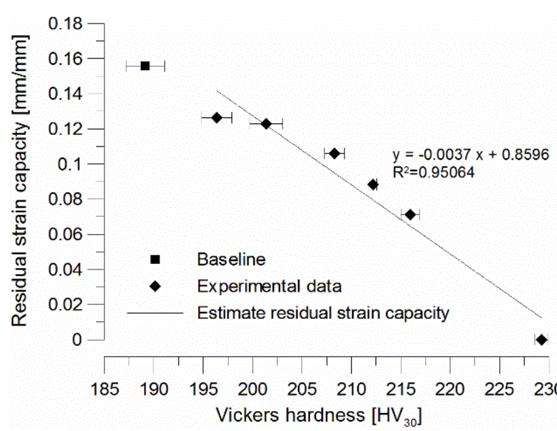

Fig. 10 Residual strain capacity versus Vickers hardness calibration curve for diameter 16 grade 430.

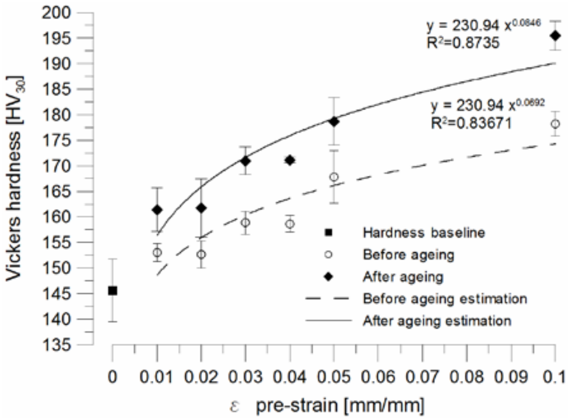

Fig. 11 Hardness versus pre-strain calibration curve for diameter 25 mm grade 300.

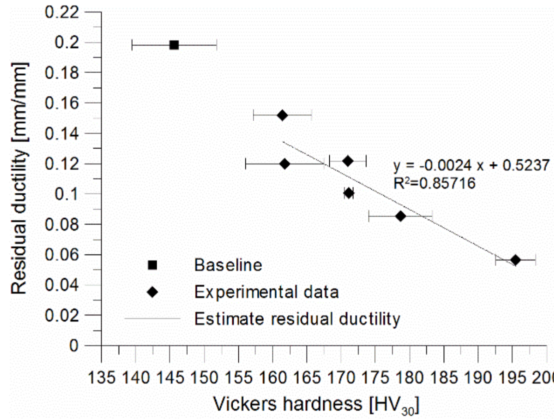

Fig. 12 Residual strain capacity versus Vickers hardness calibration curve for diameter 25 grade 300.

During the damage assessment the calibration curves were used. For bar D1, consulting the calibration curves (Fig. 9 and Fig. 10) and the maximum average hardness of 197 HV_{30}, the bar has undergone approximately 0.015 mm/mm plastic strain and the residual strain capacity predicted referred to the same location was approximately 0.13 mm/mm. Using the same approach (see Fig. 11 and Fig. 12), bar D2 was suspected to have plastically deformed about 0.03 mm/mm and the estimated residual strain capacity was 0.11 mm/mm.

In the final phase IV, in order to verify the "hardness predictions" the damaged bars were machined for tensile testing ensuring that the reduced area of the testing sample contained only the damaged material (see Fig. 7 and Fig. 8). The results of the tensile test of the damaged location (see Fig. 13 and Fig. 14), compared to the monotonic benchmark tests, showed almost no discontinuous yield stress, increased upper yield strength, increased UTS of and decreased strain at UTS: the mechanical properties of the steel changed due to the plastic deformation occurred during the earthquake (see Table 4).

The tensile test results were approximately similar with those predicted from the Vickers hardness test. The Vickers test was able to detect the damage in the bar and estimate residual strain capacity within a 25% error (Table 5).

While the material has lost ductility only over the length containing the damage, if further plastic capacity is not made available by further de-bonding from the concrete, then further elongation will be limited.

Table 4 Mechanical properties of the damaged reinforcing bars.

Bar name	**Lower Yield strength [MPa]**	**Ultimate tensile strength (UTS) [MPa]**	**Strain at UTS (%)**
D1	≈ 550	635	0.104
D2	≈ 375	536	0.136

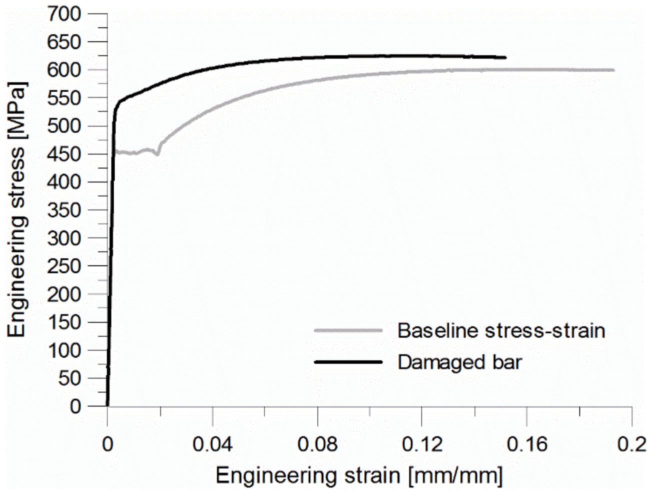

Fig. 13 Stress strain curve of the D1 damaged bar and a virgin bar of same grade and diameter.

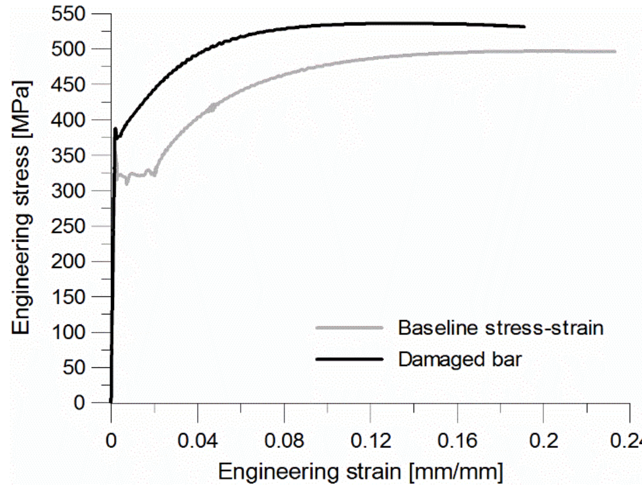

Fig. 14 Stress strain curve of the D2 damaged bar and a virgin bar of same grade and diameter.

Table 5 Comparison between predicted and actual residual strain capacity.

Bar name	**Average hardness in the damaged region [HV_{30}]**	**Predicted residual strain capacity from hardness [mm/mm]**	**Actual residual strain capacity from tensile test [mm/mm]**	**Error [%]**
D1	197	≈ 0.13	≈ 0.104	25%
D2	172	≈ 0.11	≈ 0.136	19%

7. Limitations

Although the scope of the method is to develop a non-destructive test, at this stage the Vickers hardness method is invasive, damaged reinforcing bars need to be removed from the building and taken in laboratory for hardness testing and undamaged bar lengths need to extract from the building for calibration. Further research can be focused in adopting a portable Vickers hardness tester currently available (https://www.gemeasurement.com/inspection-ndt/ultrasound/tiv).

In addition, due to the amount of work-hardening (variability of the chemical composition and thermo-mechanical history) of the various grades and even between heats and diameters of the same grades of steel, a unified calibration curve for reinforcing steel grades has not yet been developed. Therefore, in order to gain meaningful final results, calibration curves need to be developed for the specific steel of interest (e.g., grade, diameter and heat). These calibration curves are time-consuming and expensive.

Further research can also be focused on investigating the possibility to develop calibration curves based on yield strength of the material and its strain hardening exponents, in order to avoid the remove extra material for calibration curves.

The hardness method is not capable to provide the remaining fatigue life of the re-bars.

8. Summary and conclusions

The series of tests conducted at the University of Canterbury demonstrated that the Vickers hardness of the steel grades tested increases significantly and predictably with increasing plastic strain, it is then reasonable to use hardness as a key parameter to determine whether a bar has exceeded its elastic stress during a seismic event.

Because of the varying mechanical properties of steels of different manufacturing methods, origins, batches or "heats" from even a single manufacturer, the estimation of the plastic strain and residual plastic strain capacity of a bar that has been removed from a building requires calibration tests to convert hardness to plastic strain, and tensile tests to determine the original strain capacity.

Steel grades used in these experimental tests and in many buildings are prone to strain ageing. This phenomenon affects the mechanical properties of the material. Increases the yield and tensile strength after pre-strain and ageing treatment, but most significantly decreases the steel ductility. Therefore, the strain ageing effects must be included in the hardness damage assessment procedure.

The Vickers Hardness Method is able to detect the extent of plastic deformation and estimate its amount, furthermore is capable to provide indicative results in terms of residual strain capacity, as verified by tensile testing of damaged sections.

The method takes place over four distinct phases:

I. Suspected damaged reinforcing bars are removed from the building;
II. Vickers hardness tests are conducted to detect the exact location of damage on the bars;
III. If and when damage is identified, calibration curves of that specific grade and diameter of steel are produced and used to estimate damage and predict residual plastic deformation capacity;
IV. Tensile tests of the damaged location are carried out and compared to tensile test of undamaged steel from the same bar.

Acknowledgements

The authors would like to express their gratitude to the Natural Hazards Research Platform and MBIE Building System Performance Branch for financial support through the SAFER Structures Research Project; Pacific Steel for providing the steel used in this research and Holmes Solutions for the collaboration. We also acknowledge the many helpful discussions with Emeritus Professor Les Erasmus from University of Canterbury and Professor Norman Dowling from Virginia Tech.

9. References

1. Paulay, T. and M.J.N. Priestley, *Seismic design of reinforced concrete and masonry buildings*. 1992, New York: John Wiley & sons, inc.

2. Bull, D.K., *Earthquakes and the effects on structures: Some of the lessons learnt.* Australian Journal of Structural Engineering, 2013. **14**(2): p. 145-165.

3. Pampanin, S. *Reality-check and Renewed challenges in Earthquake Engineering: Implementing low-damage structural Systems–from theory to practice*. in *15th World Conference on Earthquake Engineering*. 2012.

4. Standards, N.Z., *NZS 1170.5:2004*, in *Structural design actions. Part 5: Earthquake actions - New Zealand*. 2004: Wellington, New Zealand.

5. Bradley, B.A., *Strong ground motion characteristics observed in the 4 September 2010 Darfield, New Zealand earthquake.* Soil Dynamics and Earthquake Engineering, 2012. **42**: p. 32-46.

6. Kam, W.Y., S. Pampanin, and K. Elwood, *Seismic performance of reinforced concrete buildings in the 22 February Christchurch (Lyttelton) earthquake.* Bulletin of the New Zealand Society for Earthquake Engineering, 2011. **44**(4): p. 239-278.

7. Dieter, G.E., *Mechanical metallurgy*. Vol. 3. 1976: McGraw-Hill New York.

8. Vander Voort, G.F., *Metallography: principles and practices*. 1984: ASM International.

9. Cahoon, J., W. Broughton, and A. Kutzak, *The determination of yield strength from hardness measurements.* Metallurgical Transactions, 1971. **2**(7): p. 1979-1983.

10. Matsumoto, Y., *Study on the residual deformation capacity of plastically strained steel*, in *Behaviour of Steel Structures in Seismic Areas*. 2009, CRC Press.

11. Nashid, H., et al., *Non-destructive method to investigate the hardness-plastic strain relationship in cyclically deformed steel structural steel elements.* Bulletin of the New Zealand Society for Earthquake Engineering, 2014. **47**(3): p. 181-189.

12. Allington, C., *Materials testing in buildings of interest. Gallery Apartments, Westpac centre, IRD building.* . 2011: HolmesSolution, Christchurch.

13. ASTM, *A956 - 12*, in *Standard test method for Leeb hardness testing of steel products*. 2012: West Conshohocken, PA, United States.

14. O'Neill, H., *Hardness measurement of metals and alloys*. Second edition ed. 1967: Chapman and Hall.

15. Tabor, D., *The hardness of metals*. 1951: Oxford university press.

16. Pavlina, E.J. and C.J. Van Tyne, *Correlation of Yield Strength and Tensile Strength with Hardness for Steels.* Journal of Materials Engineering and Performance, 2008. **17**(6): p. 888-893.

17. Pavlina, E. and C. Van Tyne, *Uniform Elongation and the Stress-Strain Flow Curve of Steels Calculated from Hardness Using Empirical Correlations.* Journal of Materials Engineering and Performance, 2014. **23**(6): p. 2247-2254.

18. Lee, K.-S. and J.-H. Song, *Estimation methods for strain-life fatigue properties from hardness.* International Journal of Fatigue, 2006. **28**(4): p. 386-400.

19. Hall, E., *The deformation and ageing of mild steel: III discussion of results.* Proceedings of the Physical Society. Section B, 1951. **64**(9): p. 747.

20. Baird, J., *The effects of strain-ageing due to interstitial solutes on the mechanical properties of metals.* Metallurgical Reviews, 1971. **16**(1): p. 1-18.

21. Erasmus, L. and L. Pussegoda, *Strain age embrittlement of reinforcing steels.* New Zealand Engineering, 1977. **32**(8).

22. Leslie, W.C., *The physical metallurgy of steels*. 1981, Washington.

23. Pussegoda, L.N. and L.A. Erasmus, *The effect of titanium on the strain ageing characteristics of a carbon manganese structural steel*, in *6th Australas Conf on the Mech of Struct and Mater*. 1977: Christchurch.

24. Loporcaro, G., S. Pampanin, and M.V. Kral, *Comparison between accelerated and natural strain ageing effects on New Zealand manufactured Grade 300E steel reinforcing bars*, in *NZSEE*. 2016: Christchurch.

25. Hundy, B.B., *Accelerated Strain Ageing of Mild Steel.* Journal of The Iron and Steel Institute, 1954. **178**.

26. AS/NZS, *4671:2001* in *4671:2001 Steel reinforcing materials*. 2001: Wellington, New Zealand.

27. Loporcaro, G., S. Pampanin, and M.V. Kral, *Investigating the relationship between hardness and plastic strain in reinforcing steel bars*, in *NZSEE conference*. 2014: Auckland.

28. Momtahan, A., R. Dhakal, and A. Rieder, *Effects of strain-ageing on New Zealand reinforcing steel bars.* Bulletin of the New Zealand Society for Earthquake Engineering, 2009. **42**(2).

29. Proceq, *Equotip 3 Portable hardness tester. Operating instructions*. 2007.

30. ASTM, *E8/E8M - 11*, in *Standard Test Method for Tension Testing of Metallic Materials*. 2011: West Conshohocken, PA, United States.